Green Chemistry

PAPER

View Article Online
View Journal

Published on 20 January 2025. Downloaded by Zhejiang University of Technology on 1/28/2025 6:21:55 AM.

Check for updates

Cite this: DOI: 10.1039/d4gc06142j

Metabolic engineering of *Escherichia coli* for the production of D-panthenol from 3-aminopropanol and glucose†

Junping Zhou,[a,b] Zheng Zhang,[a,b] Xinyuan Xin,[a,b] Yinan Xue,[a,b] Yihong Wang,[a,b] Xueyun Feng,[a,b] Bo Zhang,[a,b] Man Zhao,[a,b] Zhiqiang Liu *[a,b] and Yuguo Zheng [a,b]

D-Panthenol is an important chemical widely utilized in the feed, medicine and cosmetic industries. For industrial production, D-panthenol is converted by chemical condensation with 3-aminopropanol and D-pantolactone, in which D-pantolactone is produced by enzymatic racemization from chemically synthesized DL-pantolactone. In this study, the *de novo* biosynthesis of D-panthenol in engineered *Escherichia coli* from glucose with the supplementation of 3-aminopropanol was established for the first time. Upon confirmation that the D-pantothenate biosynthetic pathway could be used for D-panthenol biosynthesis, a fermentation medium and pyruvate pool of the strain were first optimized, enhancing the D-pantothenol production from 31.6 mg L^{-1} to 184.2 mg L^{-1}. Moreover, structure-guided rational protein engineering of pantothenate synthase (PS) was also applied for improving the catalytic activities towards 3-aminopropanol, variant M3 (F62L/R123Q/R189I), which destroyed the hydrogen network between the residues R123/R189 and the carboxyl group of β-alanine and showed a 3.77-fold increase in D-panthenol production compared to that of the wild-type PS. In order to enhance the supply of NADPH, genes for cofactor regeneration and the pentose phosphate pathway (PPP) were enhanced, along with the knock-down of the NADPH depletion pathway. It was found that the reduction of the *pgi* gene resulted in the enhancement of the transcription level in the PPP pathway, which led to a relatively balanced ratio of NADPH/$NADP^+$. The obtained strain DPN13 reached a peak of 1469.3 mg L^{-1} D-pantothenol in the shake flask. Fed-batch fermentation was then carried out, and the titers of D-pantoate and D-pantothenol of the final strain in a 5 L bioreactor reached 24.1 g L^{-1} and 13.2 g L^{-1}, respectively, which were the highest of biosynthesized D-pantoate and D-pantothenol reported to date. Overall, with the systematic metabolic engineering of the strain for the *de novo* biosynthesis of D-panthenol, the green production of D-panthenol with industrial sustainability would be easily achieved.

Received 4th December 2024,
Accepted 8th January 2025

DOI: 10.1039/d4gc06142j

rsc.li/greenchem

Green foundation

1. We have achieved for the first time the production of the high-value product D-panthenol by *Escherichia coli* using glucose and 3-aminopropanol as raw materials through microbial fermentation. Compared to the toxic reagents and organic solvents used in traditional chemical methods, this strategy will be more environmentally friendly.
2. The titer for D-panthenol using our strategy is the highest reported by far, reaching 13.2 g L^{-1} through a fed-batch fermentation combined strategy with systematic metabolic engineering of chassis cells and rationally engineered pantothenate synthetase with high catalytic efficiency towards an unnatural substrate, 3-aminopropanol, and is used for highly efficient D-panthenol production, laying the foundation for the industrial production of high-value D-panthenol and derivatives.
3. Specific carboxylate reductases and dehydrogenases can be screened to catalyze the reduction of endogenous β-alanine to 3-aminopropanol for self-sufficiency, enabling *E. coli* to achieve the biological production of D-panthenol using only glucose.

[a]*The National and Local Joint Engineering Research Center for Biomanufacturing of Chiral Chemicals, Zhejiang University of Technology, Hangzhou 310014, China*
[b]*Key Laboratory of Bioorganic Synthesis of Zhejiang Province, College of Biotechnology and Bioengineering, Zhejiang University of Technology, Hangzhou 310014, China. E-mail: microliu@zjut.edu.cn; Fax: +86-571-88320630; Tel: +86-571-88320379*

† Electronic supplementary information (ESI) available. See DOI: https://doi.org/10.1039/d4gc06142j

Published on 20 January 2025. Downloaded by Zhejiang University of Technology on 1/28/2025 6:21:55 AM.

1. Introduction

Panthenol is the alcohol analog of D-pantothenic acid (vitamin B_5) and is deemed as a provitamin of B_5.[1] The conformation of panthenol is divided into D-type and L-type, among which only D-pantothenol is biologically active. Besides, D-panthenol can be oxidized to D-pantothenic acid (D-PA) quickly in organisms and participate in the metabolism of coenzyme A.[2,3] In this case, D-pantothenol is often employed as a vitamin B_5 synergist and is applied as a dietary supplement in the feed industry.[4] In addition, D-panthenol is used in the pharmaceutical and cosmetic industries for its moisturizing and anti-inflammatory properties.[1,5,6] The market scale of D-panthenol continues to grow in the future along with the accelerated development of the downstream industries.

Currently, D-panthenol is chemically synthesized in the industry (route I, Fig. 1)[7] and usually synthesized by the chemical condensation of D-pantolactone ((*R*)-pantolactone) and 3-aminopropanol. Racemic pantolactones are mostly obtained by multi-step chemical reactions, including aldol–alcohol reactions between isobutyraldehyde and formaldehyde, addition of hydrogen cyanide to the resulting hydroxyaldehydes, acid hydrolysis of the resulting cyanohydrin to the corresponding carboxylic acid, and lactonization of pantoate.[8] This method is currently applied for industrial D-panthenol and D-PA production, but the needs for chemical racemization and usage of large amounts of organic reagents as well as toxic cyanide make it environmentally unfriendly, while microbial fermentation has the advantages of low cost, environmental friendliness and sustainability. Based on the gradual maturation of synthetic biology and gene editing technologies, the cycle time for the metabolic modification of microorganisms has also been greatly reduced. The construction of engineered strains for the conversion of carbohydrates to high-value chemicals is also becoming a hot research topic.[9–11]

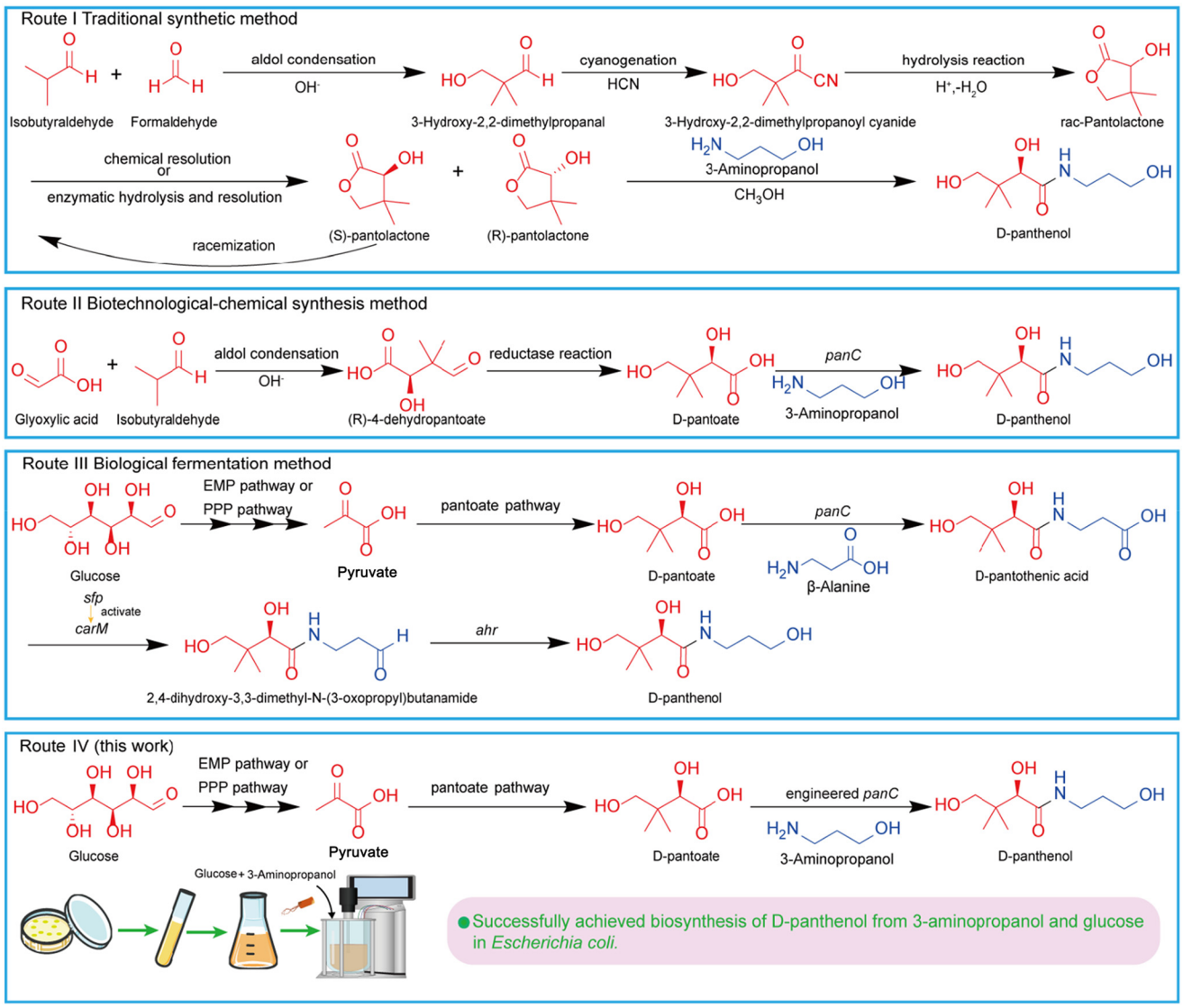

Fig. 1 Different synthesis routes to D-panthenol.

This journal is © The Royal Society of Chemistry 2025

Published on 20 January 2025. Downloaded by Zhejiang University of Technology on 1/28/2025 6:21:55 AM.

At present, many teams are focused on the biosynthesis of D-PA, but few literature studies are focused on the biosynthesis of D-panthenol by fermentation. A study has been reported for producing D-panthenol by fermentation of *Bacillus subtilis* in a medium containing D-pantoate and 3-aminopropanol, with the addition of D-pantoate as a costly substrate to the medium, and the titer of the product was only 210 mg L^{-1}.[12] Some researchers have also considered 2-hydroxy-3,3-dimethyl-4-aldehydobutyric acid as a substrate for the production of D-panthenol by microbial fermentation, but the substrate has to be produced by chemical condensation (route II, Fig. 1).[13] In addition, Lee's team proposed a very novel approach (route III, Fig. 1); since D-panthenol can be oxidized to D-pantothenic acid in living organisms, they tried to determine whether pantothenic acid could be reduced to pantothenol under the conditions of specific enzymes,[12] which involved several steps to convert pantothenic acid to aldehyde by co-expression of the carboxylic acid reductase (encoded by *carM*) and phosphopantetheinyl transferase (encoded by *sfp*); the aldehyde was reduced to D-panthenol by aldehyde reductase (encoded by *ahr*) continuously, thus eventually realizing the biologically produced D-pantoate from glucose. The final titer was 10.3 g L^{-1} in a 5 L bioreactor, which was the highest titer reported so far for the production of D-panthenol by microbial fermentation. This novel method is a pioneering work for the synthesis of D-panthenol, but, due to the difficulty of the step from carboxylic acid to aldehyde,[14,15] which limits the yield of D-panthenol and the toxic effect of aldehyde on the cells,[16] a lot of work will be needed to solve the problem. Therefore, it is also of great importance to develop a new strategy to realize the biosynthesis of D-panthenol.

Although there are few literature studies reported on the biosynthesis of D-panthenol, its derivative D-PA by fermentation has been widely reported, especially several studies covered by previous work in the lab,[17–23] which can bring us many inspirations. For example, Zhang *et al.* used *E. coli* W3110 as the starting strain to construct a chassis strain DPA9 for D-PA production with traditional metabolic modification strategies such as push–pull–block and achieved a yield of 28.45 g L^{-1} of D-PA in a 5 L bioreactor by fed-batch fermentation.[17] Subsequently, on the basis of DPA9, we determined that the phosphotransferase system was more favorable for D-PA production through CRISPRi screening and constructed the corresponding strains such as DPA11, DPA20 and DPA21, with the final strain DPA21/pBCST3 achieving a D-PA titer of 32 g L^{-1} in a 5 L bioreactor.[20] Zou *et al.* from our team knocked out *aceF* and *mdh* on the basis of strain DPA9 and increased the yield of D-PA to 68.3 g L^{-1} through optimization of the fermentation medium as well as the feed conditions.[18,19,21] Recently, the lab has also successfully increased the titer of D-PA to 97.20 g L^{-1} through strategies such as decoupling the cell growth and D-PA production of the strain, which is the highest yield reported so far.[23] In addition, other teams have also studied the production of D-PA by microbial fermentation. Song *et al.* modified the strain by the corresponding metabolic modification strategies including increasing the pyruvate pool, enhancing the D-pantoate pathway, and transporter exocytosis of the product, and finally achieved a titer of 83.26 g L^{-1} in a 5 L bioreactor.[10,24] Yuan *et al.* dynamically regulated glucose uptake to reduce overflow metabolism *via* a quorum-sensing circuit, resulting in the efficient synthesis of D-PA by *B. subtilis*, achieving a yield of 21.52 g L^{-1} in a 5 L bioreactor.[25] By learning the strategies for D-PA biosynthesis, the accumulation of a large amount of precursor D-pantoate and the highly efficient supplements of the other precursor substance 3-aminopropanol will be reasonably matched for highly efficient D-panthenol biosynthesis. Recently, it has been shown that pantothenate synthase (PS) has a broad substrate spectrum and can catalyze the condensation of β-alanine and its analogs with D-pantoate to produce the corresponding products.[26] Therefore, attempts were made to produce D-panthenol by metabolic engineering of the strain to synthesize D-pantoate from glucose and the subsequent condensation of D-pantoate and added 3-aminopropanol.

In this study, a novel route for the biosynthesis of D-panthenol from glucose and 3-aminopropanol has been established. The previously constructed strain DPA11A with highly efficient D-PA production ability was chosen as the starting strain.[27] The precursor D-pantoate was increased by various metabolic engineering strategies including increasing the pyruvate pool, enhancing the main pathway, and cofactor balancing strategies. The rate-limiting enzyme PS for the bioconversion of D-pantoate and 3-aminopropanol to D-panthenol was also facilitated by rational protein engineering. Finally, the fermentation was performed in a 5 L bioreactor for the highly efficient biosynthesis of D-panthenol.

2. Experimental

2.1. Strains and plasmids

All strains and plasmids used in this work are shown in Table S1.† *E. coli* DH5α and *E. coli* BL21(DE3) were used for plasmid constructions and protein expression, respectively. pTarget and pCas plasmids used for gene manipulations were stored in the laboratory; the antibiotics required for pTarget and pCas plasmids were spectinomycin hydrochloride (SD) and kanamycin sulphate (Kan), respectively. The pTrc99A plasmid with the Kan antibiotic requires isopropyl-beta-D-thiogalactoside (IPTG) induction for gene overexpression. The wild-type *E. coli*, *Bacillus subtilis*, *Corynebacterium glutamicum*, *Pseudomonas putida*, and *Pseudomonas aeruginosa* strains are in the laboratory collection, and are mainly used as templates for gene cloning. The starting strain DPA11A used is shown in Table S1.†

2.2. Genetic manipulations

The CRISPR-Cas9 system was employed for gene editing, knockdown and overexpression in the genome with the pCas plasmid pTarget plasmid, and the engineered clusters after knockdown were verified by colony PCR. The pTarget and pCas

Published on 20 January 2025. Downloaded by Zhejiang University of Technology on 1/28/2025 6:21:55 AM.

plasmids could be eliminated after successful gene manipulation verifications, with more details previously described.[27]

2.3. Media and culture conditions

Luria–Bertani (LB) medium containing yeast extract (5 g L^{-1}), tryptone (10 g L^{-1}), and NaCl (10 g L^{-1}) was used for seed culture, protein expression, plasmid construction, gene knockout, and strain preservation and other operations, with the addition of antibiotics such as Kan when necessary.

Shake flask fermentations were carried out in an improved MS medium (L^{-1}),[27] which contained glucose·H_2O – 25 g, $(NH_4)_2SO_4$ – 16 g, yeast extract – 3 g, KH_2PO_4 – 0.80 g, $MgSO_4$ – 0.50 g, $CaCO_3$ – 0.50 g, IPTG – 0.96 mg, and metal salt solution – 1 mL. The MS medium was sterilized at 115 °C for 30 min. Strains were inoculated into a 250 mL shake flask with 50 mL of medium and maintained at 30 °C and 200 rpm for 48 h. For shake flask fermentations, D-pantoate and D-panthenol were produced under the same conditions, except that 1.3 g L^{-1} 3-aminopropanol was added to the medium at the beginning and another 3.3 g L^{-1} 3-aminopropanol was added after 12 h for D-panthenol fermentation.

Fed-batch fermentations for the biosynthesis of D-pantoate and D-panthenol were conducted in a 5 L bioreactor, containing 1.8 L of MS medium with the initial glucose concentration kept at 20 g L^{-1}. For seed cultivations, strains were inoculated in 500 mL flasks containing 100 mL of LB medium supplemented with 50 mg L^{-1} Kan when necessary, and incubated in a rotary shaker at 200 rpm and 37 °C. Then, 200 mL of the flask culture was inoculated into a bioreactor when the seed strain OD_{600} reached 2 to 3. When the cell OD_{600} in the bioreactor reached 10, 1 mM IPTG was added for the inducible gene expressions. The incubation temperature of the bioreactor was maintained at 30 °C. The pH was adjusted to about 6.8 by using 50% ammonia, and the stirring speed of the bioreactor was adjusted from 300 rpm to 700 rpm. When the dissolved oxygen was reduced to 20%, the coupling of dissolved oxygen and agitator paddle speed was turned on to control the dissolved oxygen at 15% to 20%. Feeding solution containing 550 g L^{-1} glucose·H_2O, 2 g L^{-1} yeast extract, 10 g L^{-1} $(NH)_2SO_4$, 14 g L^{-1} KH_2PO_4, 8 g L^{-1} $MgSO_4$ and 2 ml L^{-1} metal salt solution was automatically supplied to the culture medium when the fermentation pH exceeded 6.84 due to carbon source depletion. It was worth noting that for D-panthenol fermentations in a 5 L bioreactor, additional 1.0 g L^{-1} 3-aminopropanol should be added to the initial medium, and 3-aminopropanol was also added along with the feeding medium at a constant flow rate to keep the 3-aminopropanol concentration at 1.5 g L^{-1}.

2.4. Quantitative PCR analysis

Total RNA was extracted using the FreeZol reagent (Vazyme, Nanjing, China) at 12 h during fermentation in a 5 L bioreactor. cDNA was synthesized by reverse transcription with the HiScript II Q RT SuperMix for qPCR (+gDNA wiper) (Vazyme, Nanjing, China), and transcriptional levels were measured using the ChamQ Universal SYBR qPCR Master Mix (Vazyme, Nanjing, China) with 16S RNA as the internal reference, which were shown *via* calculating the $2^{-\Delta\Delta CT}$ value. Primers for RT-qPCR are listed in Table S2.†

2.5. Quantification of intracellular NADPH/$NADP^+$

When the strain grew to the logarithmic phase in the shake flask, the solution was taken and diluted to keep OD_{600} at 0.2. Then, 1 mL of diluted solution was centrifuged and a certain amount of cell lysate was added to the precipitate. After lysis was carried out fully on ice, the mixture was centrifuged at 12 000 rpm for 5 min, and the supernatants were used for measurements using an NADPH/$NADP^+$ assay kit (Beyotime, Shanghai, China).

2.6. Site-directed saturation mutagenesis of PS

The site-directed mutagenesis of the key enzyme PanC was carried out by the rational engineering of the substrate β-alanine binding domain, in which the residues involving the contact with the carboxylate group of β-alanine were chosen, including P28, M30, L40, N58, Q61, F62, R123, H126, I133, V134, L137, K151, Q155, M178, L186, and R189. The site-directed mutagenesis was achieved by PCR, with the primers designed containing the point mutation codons and bilateral 15–20 bp homologous sequences. After the PCR and the digestions of mother plasmids using Dpn I (Takara, Beijing, China), the remaining solutions was electrotransformed into *E. coli* DPA11A with the PS gene *panC* knocked out, named DPN1. And the successful PanC variants were sequenced by Tsingke (Tsingke, Beijing, China). And these constructed strains were used for D-panthenol fermentation in shake flasks.

2.7. Analytical methods

Cell OD was monitored by measuring absorbance at a visible spectrum of 600 nm using a spectrophotometer (Mapada, Shanghai, China). For the 3-aminopropanol tolerance test, the OD_{600} of the strain was detected by using an automatic microbial adaptive evolution instrument (TianMu, Wuxi, China). And the residual glucose concentration was measured by a 3,5-dinitrosalicylic acid (DNS) assay. D-panthenol was monitored by HPLC with a UV detector (Thermo Fisher Scientific, MA, USA), using a C 18-H column (250 × 4.6 mm, 5 μm, J&K Scientific) with measuring the UV absorbance at 200 nm. The mobile phase was used at a flow rate of 0.8 ml min^{-1} and consisted of 95% water, 4.9% acetonitrile, and 0.1% phosphoric acid. The column temperature was kept at 30 °C. D-Pantoate and other organic acids were detected by using a differential refractive index detector (RID) using a Bio-Rad Aminex HPX-87H column, with the column temperature kept at 55 °C and the flow rate kept at 0.6 mL min^{-1} for 5 mmol L^{-1} H_2SO_4 as the mobile phase.[21] The RID detector temperature was kept at 40 °C. The amino acid analysis was carried out by high performance liquid chromatography (HPLC), using a C 18-H column (250 × 4.6 mm, 5 μm, J&K Scientific) with the detection wavelength kept at 338 nm and the column temperature kept at 35 °C, using the OPA pre-column derivatization method.[28]

This journal is © The Royal Society of Chemistry 2025

Published on 20 January 2025. Downloaded by Zhejiang University of Technology on 1/28/2025 6:21:55 AM.

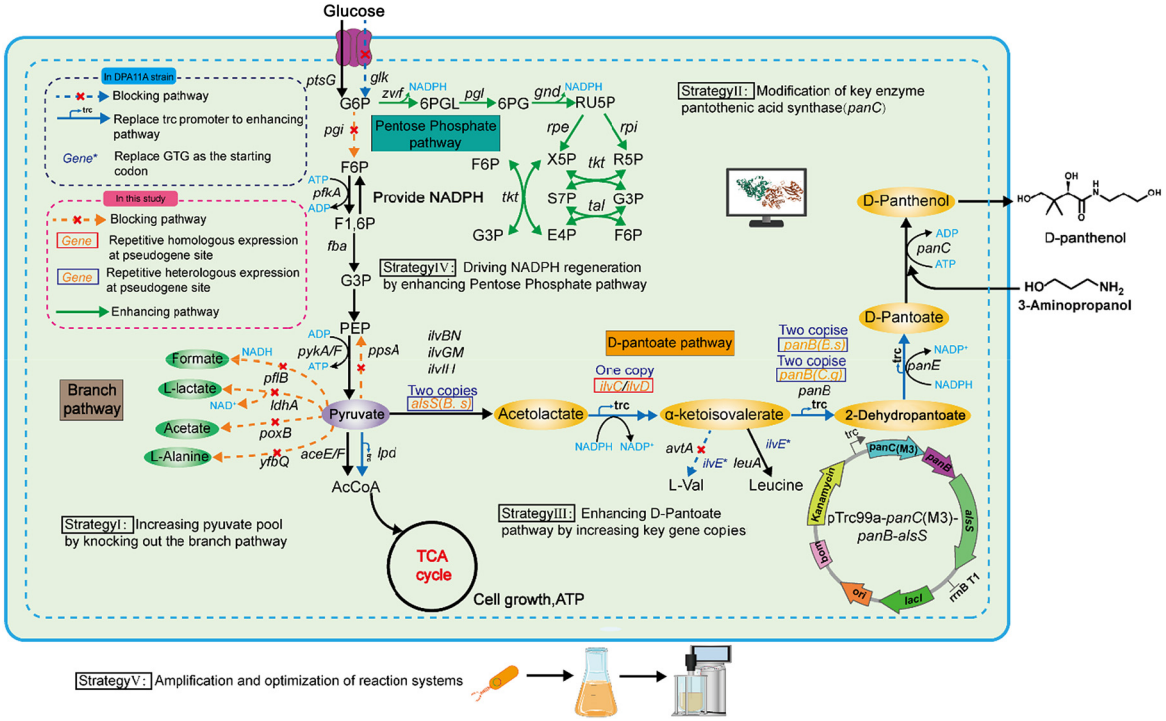

Fig. 2 Metabolic engineering of *E. coli* for the *de novo* synthesis of D-panthenol. G6P: glucose-6-phosphate, F6P: fructose 6-phosphate, F1,6P: D-fructose 1,6-bisphosphate, G3P: glyceraldehyde 3-phosphate, PEP: phosphoenolpyruvate, AcCoA: acetyl-CoA, 6PGL: 6-phospho-D-gluconate, Ru5P: ribulose 5-phosphate, X5P: xylulose 5-phosphate, R5P: ribose-5-phosphate, S7P: sedoheptulose-7-phosphate, E4P: erythose-4-phosphate, TCA cycle: tricarboxylic acid cycle.

2.8. Statistical analysis

All experiments were performed in triplicate, and the results are presented as mean ± standard deviation. A significance level of $p < 0.05$ was used. The figures were generated using Origin software version 8.0 (OriginLab Corp, Northampton, USA) and GraphPad Prism 8 (GraphPad, San Diego, CA, USA). The data represent the means of three replicates, and the error bars represent standard deviations ($*p < 0.05$; $**p < 0.01$; $***p < 0.001$).

3. Results

3.1. Introducing and engineering the D-panthenol synthesis route in *E. coli*

Endogenous pantothenate synthase (PS) of *E. coli* is a key enzyme in the D-PA biosynthesis pathway, capable of condensing D-pantoate and β-alanine for the production of D-PA, and it is now shown that it can also catalyze the condensation of β-alanine analogues with D-pantoate to generate a wide variety of valuable products, such as D-panthenol, D-pantoyltaurine and D-pantothenamides.[26,29] In this study, we evaluated the ability of *E. coli* to produce D-panthenol. In our previous study, our team constructed a strain DPA11A that is capable of highly efficient production of D-PA, and the pathway genes were strengthened using the trc promoter, and the branch metabolic pathways for synthesizing valine and isoleucine were weakened (Fig. 2). Thus, DPA11A was chosen as our initial strain. Firstly, to verify the importance of *panC* for the generation of D-panthenol, we knocked out *panC* from this strain to obtain DPN1. To serve as a control, we also introduced *panC* into DPN1 *via* ptrc99a-*panC*, and thus strains DPA11A, DPN1, DPN1-ptrc99a, and DPN1-ptrc99a-*panC* were all used for flask fermentations to confirm their abilities of D-panthenol biosynthesis, under the conditions of the supplementation of 3-aminopropanol. As shown in HPLC results (Fig. S1†), the same peak as the D-panthenol standard was detected in the fermentation broth of the strains DPA11A and DPN1-ptrc99a-*panC* by HPLC at 11.1 min. We then analysed the fermentation broth sample and the standard of D-panthenol by LC-MS (Fig. S2†). The mass spectrometry results showed that the molecular mass was kept according to that of the D-panthenol standard. While no D-panthenol was detected for the control strain DPN1 (Fig. 3A), the subsequent strain DPN1-ptrc99a-*panC* that was backfilled with *panC* by a plasmid and DPA11A could produce 31.7 mg L^{-1} and 11.2 mg L^{-1} D-panthenol, respectively. Subsequently, we also screened *panC* from different species sources (Fig. 3F) and found that endogenous *panC* from *E. coli* was the most effective.

D-Panthenol is formed by the condensation of D-pantoate and 3-aminopropanol by enzyme PS, and the concentrations of precursors usually directly affect the productions. By adding D-pantoate (Fig. 3E), the results showed that as the amount of the supplemented D-pantoate increased, the D-panthenol production increased and reached a maximum titer of 835.2 mg

Published on 20 January 2025. Downloaded by Zhejiang University of Technology on 1/28/2025 6:21:55 AM.

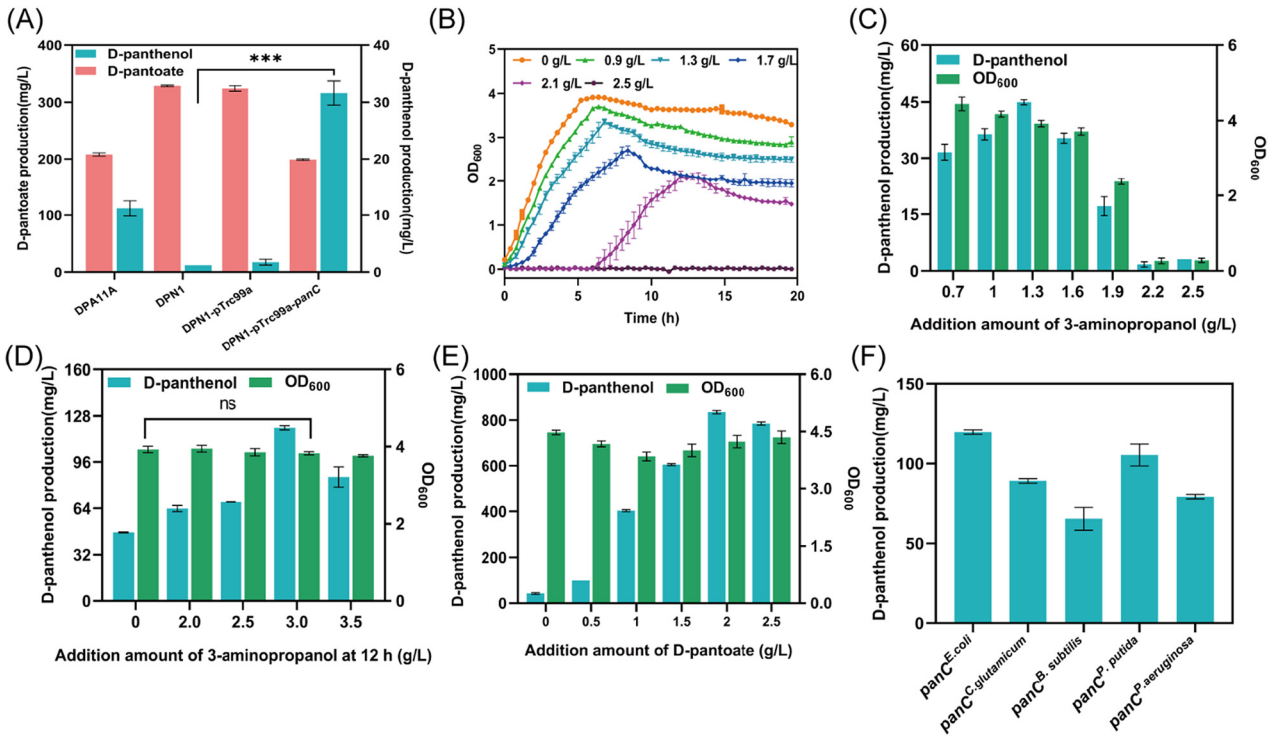

Fig. 3 Introducing the D-panthenol synthesis route in *E. coli*. (A) D-Panthenol production of the engineered strains DPA11A and DPN1 in a D-panthenol fermentation medium containing 0.5 g L^{-1} 3-aminopropanol. (B) Cell growth curves of DPA11A at different concentrations of 3-aminopropanol in LB medium. (C) Under different 3-aminopropanol addition conditions, D-panthenol and biomass (OD_{600}) were fermented for 48 h. (D) Effect of 3-aminopropanol supplementation after 24 h fermentation on D-panthenol production by DPN1-pTrc99a-*panC*. (E) Effect of exogenous addition of different concentrations of D-pantoate on D-panthenol production by engineered DPN1-pTrc99a-*panC*. (F) The experimental data for the screening of *panC* from different species. *p < 0.05, **p < 0.01, ***p < 0.001; ns, no significance.

L^{-1} when the supplemented D-pantoate concentration reached 2 g L^{-1}. Thus, the enhancement of the D-pantoate biosynthesis pathway would be useful for improving D-panthenol production. Another precursor 3-aminopropanol was found to be toxic for the cell growth (Fig. 3B), as the cell OD_{600} decreased more than 50% when the concentration of the supplemented 3-aminopropanol exceeded 1.7 g L^{-1}. Supplementation of low concentration 3-aminopropanol resulted in an insufficient supply of precursors and a low yield, while supplementation of high concentration 3-aminopropanol prevented the strain from growing normally and also led to low level D-panthenol production. We therefore optimized the conditions for 3-aminopropanol addition, including the timing and amounts. The effects of 3-aminopropanol on the production of D-panthenol by adding to the initial medium were studied (Fig. 3C), and it was found that the optimal amount of 3-aminopropanol was 1.3 g L^{-1}, which resulted in D-panthenol production of 44.9 mg L^{-1}. Subsequently, we chose to supplement 3-aminopropanol when the cell growth reached the stationary phase with cultivation times for about 12 h (Fig. 3D), and it was found that the supplementation of 3.0 g L^{-1} 3-aminopropanol at 12 h could obtain the maximum D-panthenol titer at 119.7 mg L^{-1}, about 2.77-fold higher than that of the control. It could be concluded that the two precursors were both vital for the D-panthenol biosynthesis, and how to increase the production of D-pantoate in the chassis cells had also become a key problem to be solved in this study.

3.2. Enhancing D-pantoate accumulations by knockdown of the branch pathway of pyruvate metabolism

Pyruvate is a key intermediate metabolite linking the EMP pathway and the TCA cycle, and a key node for the biosynthesis of D-panthenol and other by-products.[30–32] Pyruvate can be converted to lactate, acetic acid, ethanol, formic acid, L-alanine *etc.*, *via* the endogenous metabolic pathway in *E. coli*, in which pyruvate oxidase (encoded by the gene *poxB*) is capable of oxidizing pyruvate to acetic acid and carbon dioxide. Biosynthesis of L-alanine was achieved by the transamination reaction from pyruvate, which required three isoenzymes (encoded by the genes *yfbQ*, *yfdZ*, and *avatA*). The phosphoenol-pyruvate synthetase (encoded by *ppsA*) catalysed the formation of phosphoenolpyruvate and ADP from pyruvate and ATP. In addition to the above enzymes, there were also D-lactate dehydrogenase (coded by *ldhA*) and phosphoheptulonate synthase (coded by *aroG*), all of which were involved in the branch pathway of pyruvate metabolism.[11,33–35] By knocking down the pyruvate branch pathway, the pyruvate pool would be improved, which often led to the enhanced titer of the target products derived from pyruvate.[10,36] The versatile C4 platform molecule 2,4-dihydroxybutyric acid showed 10-fold higher titer than that of

This journal is © The Royal Society of Chemistry 2025

Published on 20 January 2025. Downloaded by Zhejiang University of Technology on 1/28/2025 6:21:55 AM.

the control group, after the knockdown of genes *poxB*, *pflB* and *adhE*.[11] The production of D-PA could also be promoted by 52.12% after increasing the pyruvate pool.[10] Using the same strategy for enhancing D-pantoate biosynthesis by increasing the pyruvate pool, D-panthenol production could also be enhanced.

Firstly, we analyzed the accumulated heteroacids during fermentation for the starting strain DPA11A by HPLC (Table S3†); it was found that the strain showed heteroacid accumulations and produced less than 0.5–1 g L^{-1} acetate, formate, L-alanine, and lactate. On this basis, single gene knockdowns of these selected branch metabolic genes *poxB*, *ppsa*, *pflB*, *yfbQ*, *ldhA* and *aroG* were verified (Fig. 4A), and the results showed that D-pantoate production could be improved by these gene deletions. Therefore, the cumulative knockout of these genes was carried out, and the engineered strains DPN2, DPN3, DPN4, DPN5 and DPN6 were used for the shake flask fermentations of D-pantoate (Fig. 4B) and D-panthenol (Fig. 4D). The results showed that 500.9 mg L^{-1} D-pantoate was produced for DPN5, which was increased by 61.3% compared with that of the control strain DPN1. At the same time, the contents of heteroacids also showed an obvious decrease, in which the contents of acetate, formate, and L-alanine were only at 0.23–0.36 g L^{-1} (Table S3†). After the introduction of the plasmid for *panC* overexpression in DPN6, its D-panthenol titer reached 184.2 mg L^{-1}, 54.7% higher than that of the control strain DPN1 with the plasmid for *panC* overexpression. As shown in Fig. 4B and D, with the increase of D-pantoate production by the knockdown of the branch pathway of pyruvate metabolism, D-panthenol production could also be enhanced with the supplementation of 3-aminopropanol, which was in line with the conclusions obtained previously.

3.3. Modification of the key enzyme PS

The precursor pyruvate pool could be improved by the knockdown of the branch pathway of pyruvate metabolism, which help improve the D-pantoate production. However, compared with highly efficient D-PA production from our starting strain, the titer for D-pantoate production was still rather low. Considering the unnatural substrate 3-aminopropanol for enzyme PS that might lead to low enzymatic activities, the rational engineering of PS for improving catalytic efficiencies towards 3-aminopropanol would be meaningful for enhancing D-panthenol production.

PS belonged to the cytidyl transferase superfamily, and existed as a homodimer.[37] During the enzymatic catalysis process, an amide bond is formed between the amino group of β-alanine and the carboxyl group of D-pantoate, while the carboxyl group of β-alanine serves mainly for the binding of the protein.[38] So to enhance the catalytic efficiencies of PS towards 3-aminopropanol rather than β-alanine, docking analysis was conducted using one subunit of PS (Fig. S4†), and residues that could affect the binding of the β-alanine were chosen, especially the residues responsible for the binding of the carboxylate group of β-alanine, including P28, M30, L40, N58, Q61, F62, R123,

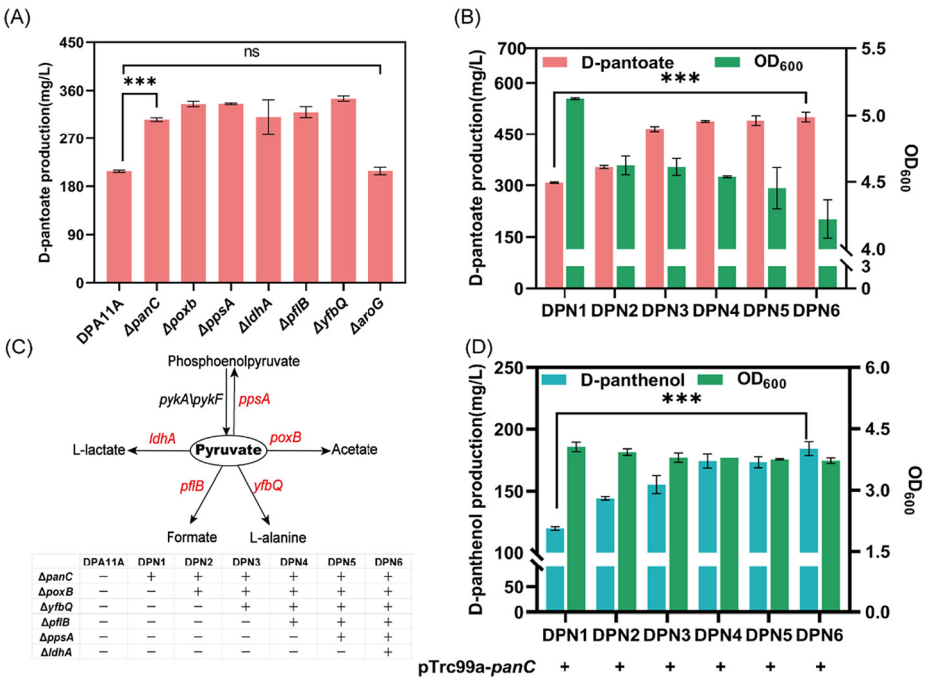

Fig. 4 Boosting pyruvate supply to promote D-panthenol synthesis. (A) Effect of single gene knockout of the pyruvate degradation pathway on D-pantoate production. (B) Effect of superimposed knockdown of the pyruvate degradation pathway on D-pantoate production. (C) Pyruvate degradation pathway and related genes. (D) Effect of superimposed knockdown of the pyruvate degradation pathway on D-panthenol production. *panC*: gene encoding pantothenate synthetase, *poxB*: gene encoding pyruvate oxidase, *ppsA*: gene encoding phosphoenolpyruvate synthetase, gene encoding *ldhA*: gene encoding D-lactate dehydrogenase, *pflB*: gene encoding pyruvate formate-lyase, *yfbQ*: gene encoding glutamate-pyruvate aminotransferase, *aroG*: gene encoding 3-deoxy-7-phosphoheptulonate synthase. *$P < 0.05$, **$P < 0.01$, ***$P < 0.001$; ns, no significance.

Published on 20 January 2025. Downloaded by Zhejiang University of Technology on 1/28/2025 6:21:55 AM.

H126, I133, V134, L137, K151, Q155, M178, L186, and R189. Alanine scanning strategy was applied for the mutagenesis of these residues, and the results are shown in Fig. 5A. The results showed that the alanine substitutions for residues F62, R123, and R189 had positive impacts on the improvement of D-panthenol production, and the D-panthenol titers for variants F62A, R123A, and R189A were 8%, 41%, and 21% higher than those of the wild type (WT), respectively. Subsequently, residues F62, R123, and R189 of PS were chosen for saturation mutations (Fig. S6†). Among the variants for saturated mutagenesis, variants F62I, F62 M, R123Q, R123N, and R189I showed 260.0, 238.9, 263.9, 253.2, and 269.0 mg L^{-1} D-panthenol production, respectively, higher than 176.6 mg L^{-1} D-panthenol production for WT. Later, these useful variants were chosen for double-point and triple-point combination mutations, and the results are shown in Fig. 5C and D. For double-point combination mutations, variants R123Q/R189I and R123A/R189I showed 515.2 and 383.7 mg L^{-1} D-panthenol production, 191.7% and 117.3% higher than that of WT, respectively. And for triple-point combination mutations, variant F62I/R123Q/R189I, named M3 here, showed 653.5 mg L^{-1} D-panthenol production, which was 3.77 times that of the WT.

The specific activity and conversion rate of M3 were also determined, as shown in Fig. S7.† By homologous modelling

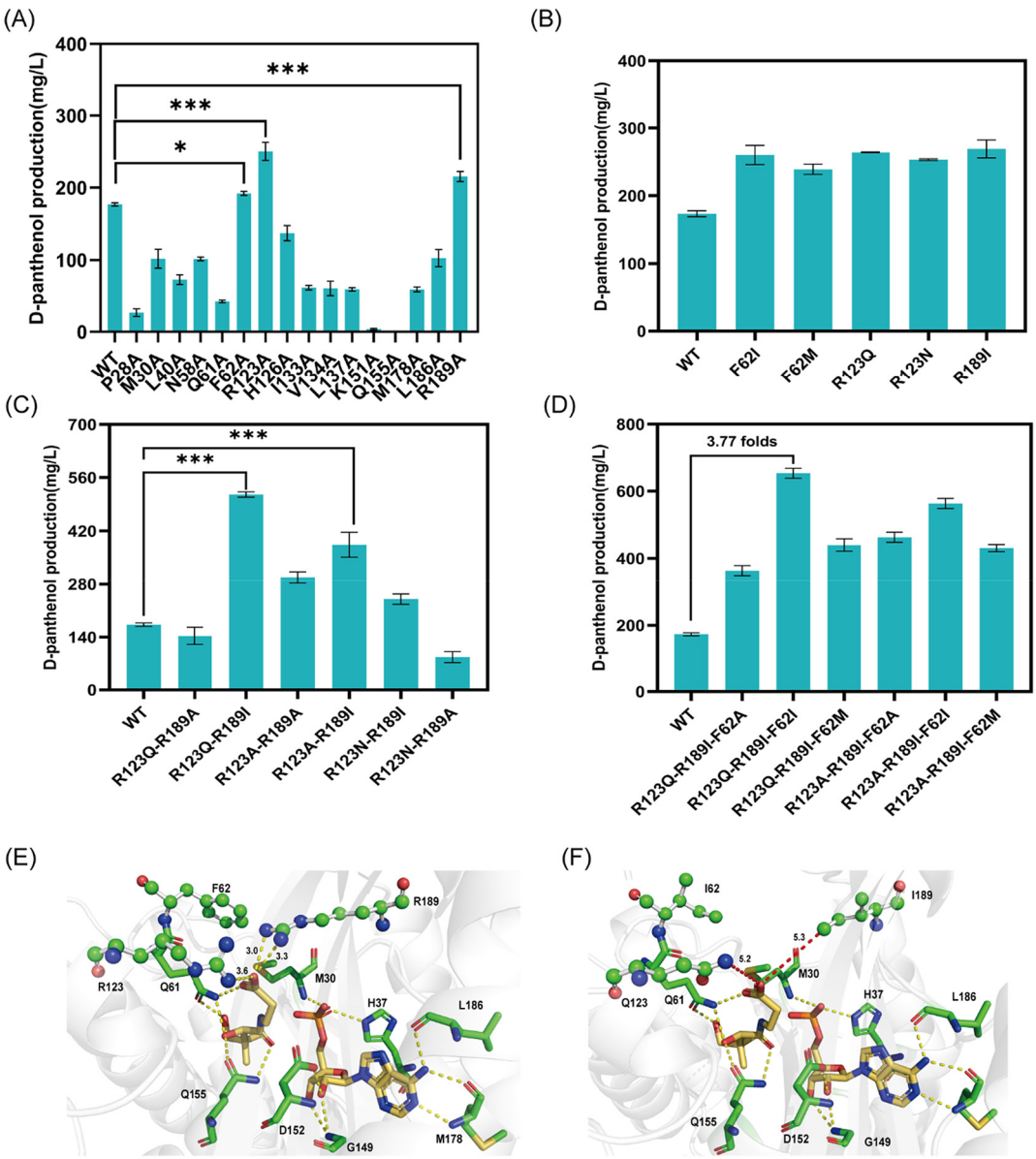

Fig. 5 Activity and the effect of PS and its mutants on D-panthenol production. (A) Effect of the active pocket alanine scanning strategy on the yield of D-panthenol. (B) The evaluation of mutants from site-saturation mutagenesis. (C) The evaluation of double mutants. (D) The evaluation of triple mutants. (E) Schematic representation of the interactions between the substrate and PS based on PDB 3UY4. (F) Schematic representation of the interactions between the substrate and M3 based on PDB 3UY4.

This journal is © The Royal Society of Chemistry 2025

Published on 20 January 2025. Downloaded by Zhejiang University of Technology on 1/28/2025 6:21:55 AM.

using a Swiss model, the enzyme template – PDB: 3uy4 – with ligand binding was chosen, as a precise PS structure model needed to be constructed on the basis of a closed conformation template for this enzyme was reported to transform its open conformation into a closed one during catalysis.[37] It was found that R123 and R189 could directly form hydrogen bonds with the hydroxyl group of the D-pantothenate carboxylate group, while the residue Q61 formed hydrogen bonds with the carbonyl group of the D-pantothenate carboxylate group and the hydroxyl group adjacent to the amido group. By the substitutions of Q61 with L-alanine, the binding of the substrate 3-aminopropionic acid would be largely affected, thus the variant Q61A showed only 23.9% D-panthenol production compared with that of wild type PS (Fig. 5A). For the mutagenesis of R123 and R189, the original hydrogen bonds with the hydroxyl group of the D-pantothenate carboxylate group were disrupted, which could make sure that the substrate specificity towards β-alanine was unfavoured, and the changed side chain structure for variants R123N and R189I would be beneficial for D-panthenol production. With the synergistic effect of the introduction of F62I mutagenesis, the constructed precise substrate binding domain of M3 would be more suitable for the catalysis of the substrate 3-aminopropanol. It is reported that the disruptions of the hydrogen network between the residues and the substrate fumaric acid of aspartase can make the enzyme catalyze different types of unnatural aliphatic and aromatic olefin acids to the corresponding β-amino acids.[39] And our strategy for the disruptions of the hydrogen network also achieved high catalytic efficiencies of PS on the unnatural substrate 3-aminopropanol.

We then used molecular dynamics simulations to study the mechanism of enzyme activity enhancement (Fig. S5†). The results of root mean square fluctuation (RMSF), reflecting the flexibility of the protein residues and domains, showed that PS loop with residue 60–80 of variant M3 was much more flexible than that of the wild type PS. This indicated that the substitutions in variant M3, especially for the substitution of F62 with Ile, largely improved the flexibilities of this loop, which might be responsible for the substrate entrance and binding. The improved loop flexibilities could help enhance the enzymatic activities by improving the 3-aminopropanol entrance rate and the dissociation rate of the product D-panthenol. At the same time, residue 189 located at the rigid α-helix domain, with the substitution of R189 with Ile, the RMSF value for this α-helix was largely decreased, indicating that the introduction of a hydrophobic amino acid for residue 189 could enhance the rigidity of the α-helix domain, which was beneficial for the substrate binding and catalysis. Thus, compared with wild type PS, variant M3 could show higher catalytic efficiencies and stabilities towards the substrate 3-aminopropanol, resulting in 3.77-fold improvement for D-panthenol production.

3.4. Screening and overexpression of D-pantoate synthesis pathway genes

The knockdown of the heteroacid biosynthesis pathway and modification of the key enzyme led to an increase in the titer of D-pantoate and D-panthenol, but the accumulation of pyruvate, an intermediate of strain DPN6, was still high (Table S3†). In order to convert the over-accumulated pyruvate to D-pantoate and D-panthenol, the overexpressions of the pathway genes for converting pyruvate to D-pantoate were further enhanced (Fig. 6).

The acetolactate synthase of *B. subtilis* (encoded by *alsS*) has been widely overexpressed to increase the production of D-PA and its derivatives, because it is not affected by endogenous feedback inhibition in *E. coli*.[40] We introduced *alsS*, *ilvC* and *ilvD* tandem genes with a strong promoter trc into DPN6 to obtain DPN7 (Fig. 6A). DPN7-pTrc99a-M3 showed enhanced the production of D-panthenol to 705.1 mg L^{-1}, and the D-pantoate production by DPN7 reached 747.1 mg L^{-1} (Fig. S8†), 50.7% higher than that of DPN6. Meantime, the integration of a single *alsS* gene into the genome of DPN7 was carried out to obtain DPN8, and this strain showed increased D-panthenol production to 735.3 mg L^{-1}, with the accumulation of pyruvate decreasing to 1.32 g L^{-1}. Subsequently, another copy of *alsS* was integrated into the genome to obtain DPN8-1, but unfortunately, the titer of D-panthenol was not significantly improved. Ketopantoate was generated from α-ketoisovalerate by *panB* with the important one-carbon unit donor supply of the folate cycle. Thus, the intracellular one-carbon unit carrier is also critical for D-pantoate synthesis. It has been documented that *serA* and *glyA* genes, key genes in the serine pathway, can be studied to promote the biosynthesis of serine and methylenetetrahydrofolate.[41,42] Therefore, *serA* and *glyA* genes under the trc promoter were integrated into the genome to obtain DPN8-2. Unfortunately, no positive results were achieved. The gene *panB* has been studied for the enhancement of D-PA biosynthesis, in which *panB* from *C. glutamicum* and *panB* from *B. subtilis* were previously studied in our lab,[17] so *panB* from *C. glutamicum* and *panB* from *B. subtilis* were both overexpressed in DPN8 to obtain DPN12. The results showed that with the increase of the copy numbers of *panB*, the D-panthenol production increased gradually (Fig. 6A). The D-pantoate titer and D-panthenol titer of the strain DPN12 reached 1001.6 mg L^{-1} and 1075.1 mg L^{-1}, respectively, while the accumulation of pyruvate decreased to 0.75 g L^{-1}. We then tried to increase the copies of *panE* in the DPN12 genome to obtain DPN12-1, but the results showed that increasing the copies of *panE* had no positive effect on D-panthenol and D-pantoate productions. Overall, the overexpressions of D-pantoate pathway genes in the genome of the strain DPN6 to obtain DPN12 showed 52% increased D-panthenol production, which further illustrated the importance of enhancing the D-pantoate pathway for driving the carbon flux to D-PA and its derivative productions.

To consider the effects of further overexpressions of these key genes on D-panthenol productions, several pathway genes were overexpressed by the pTrc99a plasmid. Furthermore, other sources for *panB* were also considered, and the fermentation results of D-panthenol (Fig. 6B) and D-pantoate (Fig. S8†) were analyzed. The results showed that the *alsS* gene and the *panB* gene (from *P. putida*) had positive effects on D-pantoate

Published on 20 January 2025. Downloaded by Zhejiang University of Technology on 1/28/2025 6:21:55 AM.

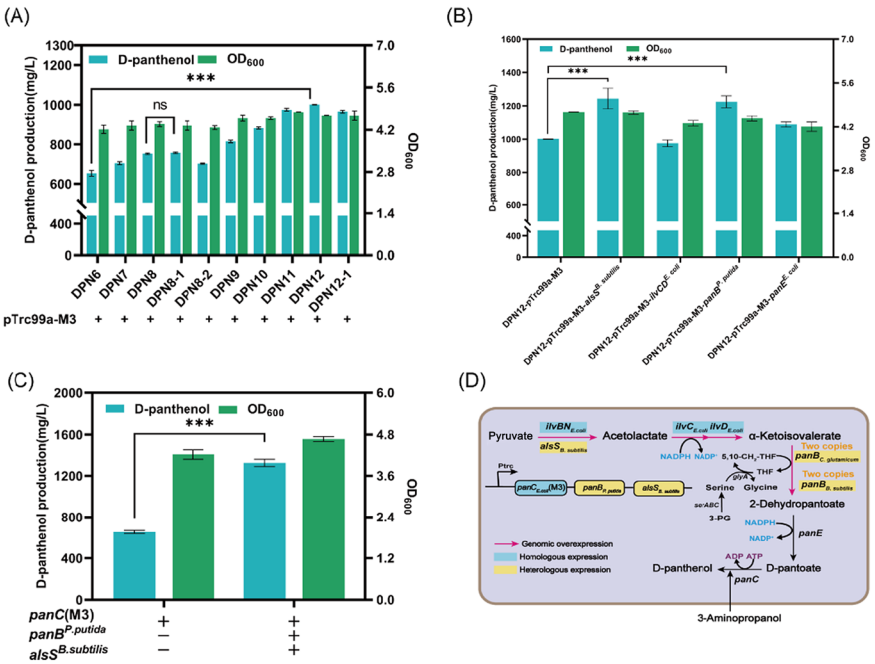

Fig. 6 Enhancement of the D-pantoate pathway to increase D-panthenol production. (A) Effects of increasing D-pantoate pathway genes in the genome on D-panthenol production. (B) Effect of the overexpression of the pantoate pathway gene through plasmid pTrc99a on D-panthenol production. (C) Effect of the overexpression of *panB* and *alsS* by plasmid pTrc99a on D-panthenol production. (D) Overview of the D-pantoate pathway for the synthesis of D-panthenol. 3-PG: 3-phosphoglycerate. **P* < 0.05, ***P* < 0.01, ****P* < 0.001; ns, no significance.

and D-panthenol productions, and then co-expressions of both genes in tandem with M3 in a single plasmid were carried out to obtain the plasmid pTrc99a-M3-*panB*$^{P.\ putida}$-*alsS*$^{B.\ subtilis}$, named pTrc99a-CBS. The results showed that D-panthenol production for the strain DPN12-pTrc99a-CBS reached 1375.2 mg L^{-1}. We also performed shake flask fermentation of D-pantoate using the pathway gene overexpression plasmid pTrc99a-*panB*$^{P.\ putida}$-*alsS*$^{B.\ subtilis}$ (pTrc99a-BS) which did not carry M3 (Fig. S8†), and this strain showed the highest D-pantoate titer of 1364.1 mg L^{-1}.

3.5. Promoting strain growth and product synthesis by increasing redox fluxes

A more favourable intracellular redox homeostasis process not only contributes to good cell growth, but also to the synthesis of metabolites, including squalene, L-5-hydroxytryptophan, xylitol and other industrially valuable products.[24,43–45] Two molecules of NADPH are employed for the biosynthesis of one molecular D-pantoate from pyruvate. NADPH is consumed by ketol-acid reductoisomerase (encoded by *ilvC*) and 2-dehydropantoate 2-reductase (encoded by *panE*). Therefore, for the efficient synthesis of D-pantoate, the supply of NADPH is also one of the key factors that limit the production of D-pantoate and D-panthenol. Strategies for the balance of NADPH to $NADP^+$, along with the sufficient supply of NADPH include enhancing the PPP pathway, changing the enzymatic cofactor specificities for NADH, replacing the pathway NADPH-dependent enzymes with NADH-dependent enzymes, overexpression of NADPH regeneration enzymes, like glucose dehydrogenase (encoded by *gdh*), pyridine nucleotide transhydrogenase (encoded by *pntAB*) and the $NADP^+$-dependent glucose-6-phosphate dihydrogenase (encoded by *zwf*), and reducing the consumption of NADPH by knocking out NADPH-consuming enzymes.

In this study, we tried three ways to maintain the intracellular redox homeostasis; firstly, we overexpressed NADPH regeneration enzymes genes, *zwf*, *gnd* and *pntAB*, on the basis of DPN12, and the fermentation processes for D-pantoate (Fig. S9†) and D-panthenol (Fig. 7A) production were carried out. It could be found that the biomass increased after the overexpression of NADPH-producing enzymes, and the NADPH/$NADP^+$ ratio was also increased in the strains with these enzyme overexpressions (Fig. 7C). These results confirmed that improved redox homeostasis contributed to the good cell growth of the strains. Among these strains, the engineered strain with *zwf* overexpression showed the highest production of D-panthenol and D-pantoate, which reached 1385.1 mg L^{-1} and 1415 mg L^{-1}, respectively. In addition, strengthening of the PPP pathway was also carried out by knocking out the *pgi* gene, and it was found that the production of D-panthenol reached 1460.3 mg L^{-1} and the OD_{600} increased from 4.7 to 5.5 after the *pgi* knockout. Meanwhile, the production of D-panthenol also reached 1460.3 mg L^{-1} for this strain. Then, RT-qPCR experiments for the genes related to the PPP pathway were conducted (Fig. 7B), and results showed that all the transcriptional levels of the PPP pathway genes were strengthened compared with that of the control, in which the transcriptional levels of the *zwf* gene was 6.13-fold higher than that of the control group. This further showed the

 This journal is © The Royal Society of Chemistry 2025

Published on 20 January 2025. Downloaded by Zhejiang University of Technology on 1/28/2025 6:21:55 AM.

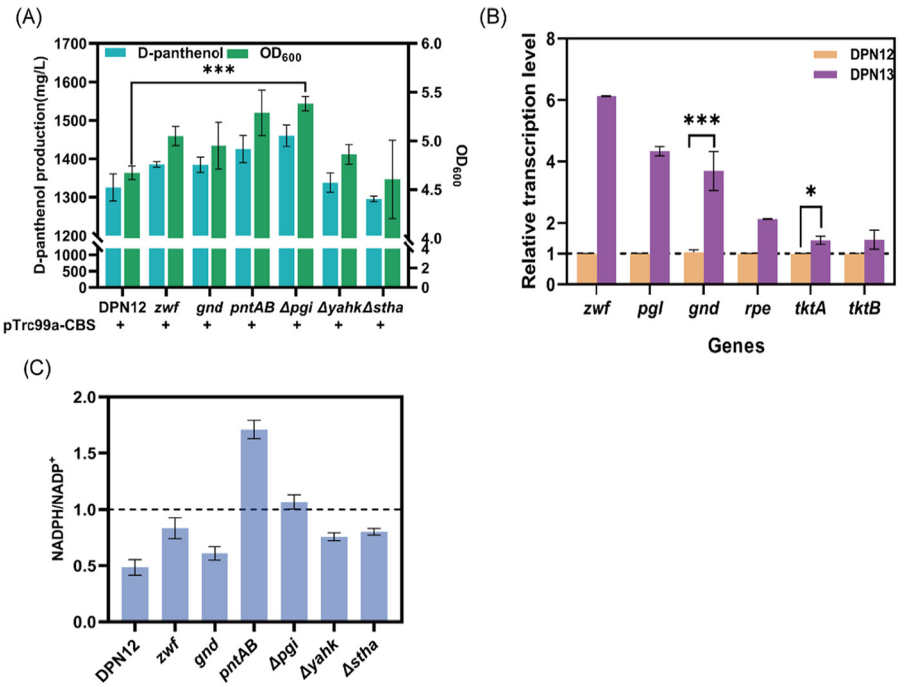

Fig. 7 A fine ratio of NADPH and $NADP^+$ in cells promotes cell growth and D-panthenol synthesis. (A) Effects of the overexpression of NADPH-generating genes and knockout-depleting genes on D-panthenol production. (B) Relative transcription level of genes related to PPP pathways between DPN12 and DPN12Δ*pgi* by RT-qPCR analysis. (C) The intracellular NADPH/$NADP^+$ ratio of the differently engineered strains. The dashed line indicates that the ratio is one. *zwf*: gene encoding $NADP^+$-dependent glucose-6-phosphate dehydrogenase, *gnd*: gene encoding 6-phosphogluconate dehydrogenase, *pntAB*: gene encoding pyridine nucleotide transhydrogenase, *pgi*: gene encoding glucose-6-phosphate isomerase, *yahk*: gene encoding aldehyde reductase, *stha*: gene encoding soluble pyridine nucleotide transhydrogenase. *$p < 0.05$, **$p < 0.01$, ***$p < 0.001$; ns, no significance.

critical role of *zwf* for D-panthenol production. We also knocked out *yahK* (encoding aldehyde reductase) and *sthA* (encoding soluble pyridine nucleotide transhydrogenase), which were considered as NADPH depleting enzymes. As shown in Fig. 7A, flask fermentation results showed that the productions of D-pantoate and D-panthenol were not significantly enhanced for *yahK* and *sthA* knockdown. The strain DPN13, named with the *pgi* knockout based on the strain DPN12, was further used for *zwf*, *gnd*, and *pntAB* overexpression (Fig. S9†). Unfortunately, although the intracellular NADPH/$NADP^+$ ratio for these strains was higher than that of DPN13, the D-pantoate titer and D-panthenol titer were lower, which further indicated that balanced redox homeostasis had positive effects on the metabolite production and cell growth. Any unbalanced redox homeostasis would affect the cell growth and final product titer.

3.6. Fermentation processes for highly efficient D-panthenol production in a 5 L bioreactor

Fed-batch fermentation is an effective way to evaluate whether the strain can be truly applied to industrial production. Here, the strain DPN13-pTrc99a-M3-$panB^{P.\ putida}$-$alsS^{B.\ subilis}$ was used for fed-batch fermentation processes in a 5 L bioreactor with 2 L liquid volume to evaluate its D-panthenol production capacity (Fig. 8). Prior to this, the fermentation of DPN13-pTrc99a-$panB^{P.\ putida}$-$alsS^{B.\ subilis}$ in a 5 L bioreactor was also evaluated for D-pantoate production. During the fermentation process, the glucose concentration was controlled to be less than 5 g L^{-1}, and the dissolved oxygen was controlled to be between 15% and 20%. The highest titer of D-pantoate reached 24.1 g L^{-1} after 72 h fed-batch fermentation, which was the highest titer for D-pantoate reported by far.

For D-panthenol production with the strain DPN13-pTrc99a-M3-$panB^{P.\ putida}$-$alsS^{B.\ subilis}$ in a 5 L bioreactor, the strategy and medium of the fermentation were almost the same as those for D-pantoate fermentation. Moreover, 3-aminopropanol had been found to be cytotoxic for cell growth previously; thus, the amounts and time for 3-aminopropanol supplementation were optimized. At the beginning of the fermentation process, 1 g L^{-1} 3-aminopropanol was added to the initial medium, and after 12 h of fermentation, supplementation of 3-aminopropanol in the fermentation broth was done every 12 h to control the total 3-aminopropanol concentration at 1.5 g L^{-1}. Eventually, the titer of D-panthenol reached a maximum of 13.2 g L^{-1} at 84 h of fermentation. This was the highest D-panthenol titer obtained so far, with the *de novo* biosynthesis strategy from substrate glucose and 3-aminopropanol.

4. Discussion

D-Panthenol is a commercially valuable chemical used as provitamin B5 in food, pharmaceutical, feed and cosmetic appli-

Published on 20 January 2025. Downloaded by Zhejiang University of Technology on 1/28/2025 6:21:55 AM.

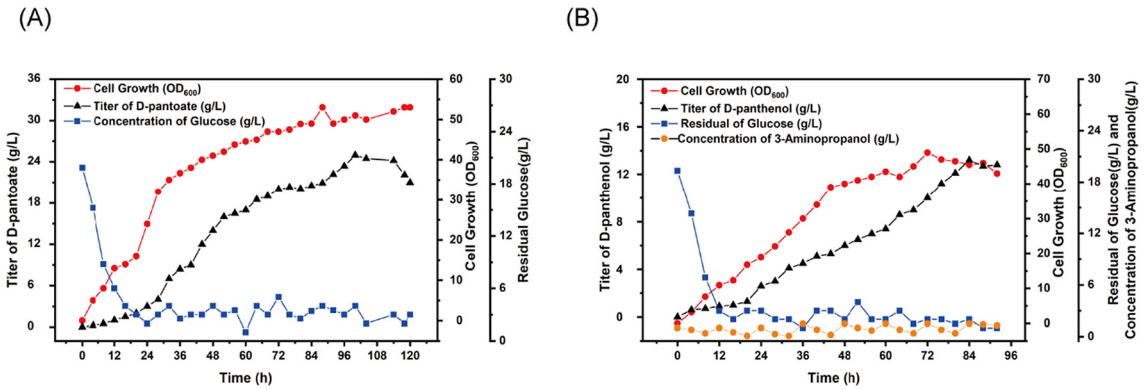

Fig. 8 Fed-batch fermentation results of DPN13-pTrc99a-BS and DPN13-pTrc99a-CBS strains in a 5 L bioreactor. (A) Results of D-pantoate production by fermentation of the engineered strain DPN13-pTrc99a-BS in a 5 L bioreactor for 120 h. (B) Results of D-panthenol production by fermentation of the engineered strain DPN13-pTrc99a-CBS in a 5 L bioreactor for 120 h.

cations, and its precursor D-pantoate is also of high commercial value as a precursor for the synthesis of D-PA. The production of D-panthenol by microbial fermentation is a revolutionary method for the replacement of traditional chemical production. In this study, a highly efficient *E. coli* cell factory was constructed for the first time to produce D-panthenol by co-fermentation of glucose and 3-aminopropanol. Meanwhile, the key enzyme PS, which had been reported for a wide substrate spectrum,[26] was also studied for improving D-panthenol production. Considering the unnatural 3-aminopropanol substrate that was not suitable for PS enzyme binding, the precise residues binding the carboxylate group of β-alanine were modified accordingly in this study. With rational engineering for reducing the hydrogen bonds with the β-alanine carboxylate group, variant M3 (F62L, R123Q and R189I) was successfully constructed and showed a 3.77-fold increase for D-panthenol production compared with the overexpression of the wild-type PS in DPN6. Although the present study only focused on the production of D-panthenol, it could be speculated that the rational engineering of PS would be beneficial for the biosynthesis of D-PA and its derivatives. As the derivatives of D-PA have been used for the synthesis of antibiotics and other chemicals,[46,47] the subsequent modification and application of PS may also become a hot issue in the future studies.

In order to improve D-panthenol production, the sufficient supply of its precursor D-pantoate was essential. By systematic metabolic engineering including increasing the pyruvate pool, enhancing the expressions of pathway genes for D-pantoate production, and the redox balance, the D-pantoate production was greatly enhanced, which in turn further improved D-panthenol production. It was worth noting that the subsection on intracellular redox homeostasis was important, in which the PPP pathway was enhanced by knocking out *pgi*. The deletion of *pgi* in DPN12 showed enhanced reducing power, which resulted in improved cell growth and D-panthenol production. However, with the *pgi* gene deletion, it is reported that the growth of the strain will be inhibited.[48–51] We then tried to knock out *pgi* alone using wild type *E. coli* and found that the cell growth was inhibited, which was consistent with the literature. These results demonstrated the importance of intracellular redox homeostasis for the growth of the strain. The constructed strains DPN13-pTrc99a-BS and DPN13-pTrc99a-CBS were also applied for shake flask fermentations. The titers of D-pantoate and D-panthenol for two strains reached 1385.1 mg L^{-1} and 1460.3 mg L^{-1}, respectively, which were the highest titers achieved by shake flask fermentations using microbial fermentation methods.

Compared with the traditional chemical methods, the microbial fermentation method was deemed as greener and more environmentally friendly. Although only glucose was used as our fermentation substrate, by exploring the substrate with other renewable sources such as starch, cellulose hydrolysate and so on, the production of D-panthenol would not solely rely on the petrochemical industry. However, it showed a long way for the industrial applications of D-panthenol production using the microbial fermentation method, as the conversion rate for the constructed strain was only 2.16% from glucose. Thus, subsequent studies to further improve the titer and conversion rate of D-panthenol through the corresponding strategies were needed. The toxicity of 3-aminopropanol, which we encountered during the fermentation processes, was relieved by optimizing the supplementation strategies in this study. And the widely studied adaptive evolution of strains for toxic chemical tolerance[52–54] could be further used in the hope of improving the tolerance of 3-aminopropanol for our strains. Corresponding adaptive evolution experiments were also performed here in microbial microdroplet culture (MMC), and shake flask fermentations were verified but without positive results (Fig. S10 and Fig. S11†), which could be probably due to the fact that the adaptive evolution experiments for enhancing 3-aminopropanol tolerance did not favor the production of the target product D-panthenol. And these studies are still underway by using comparative transcriptomics and other methods. As for the studies of alcohol toxicities, many researchers have found that alcohols might damage the cell

 This journal is © The Royal Society of Chemistry 2025

Published on 20 January 2025. Downloaded by Zhejiang University of Technology on 1/28/2025 6:21:55 AM.

membrane, resulting in the efflux of ions from the cell, which leads to the reduction of cell activity and even cell death.[55–57] Thus, subsequent research could focus on modifying the cell membrane to improve the tolerance of 3-aminopropanol and D-panthenol production. The efficient exocytosis of the unnatural product D-panthenol by screening and improving the specific efflux protein could also increase D-panthenol production, which would be carried out in our further studies. In addition, the two-stage fermentation strategy has been reported as a useful strategy for promoting cell growth and target product biosynthesis.[10,23] Usually, the optimal conditions suitable for cell growth are established at first, and then when the strain grows to the plateau stage, the fermentation conditions are changed to make the strain produce the target chemicals. This strategy could also be explored in our further studies.

Overall, this study developed a new green *de novo* biosynthesis pathway for D-panthenol production by engineering *E. coli* from glucose and a 3-aminopropanol substrate. The efficient production of D-panthenol was achieved by increasing the pyruvate pool, rational design and modification of the key enzyme PS, enhancing the D-pantoate pathway, and the improved redox balance strategy. Finally, we carried out the 5 L bioreactor fermentation experiments to produce D-pantoate and D-panthenol by using the constructed strains, DPN13-pTrc99a-BS and DPN13-pTrc99a-CBS. And the D-pantoate titer under the fed-batch fermentation reached 24.1 g L^{-1}, while the D-panthenol titer reached 13.2 g L^{-1}, both of which are the highest titers reported so far for the production of D-pantoate and D-panthenol using microbial fermentation methods. With further applied strategies underway, including the adaptive evolution, enhancement of the D-panthenol efflux protein, and so on, the D-panthenol titer and conversion rate from glucose or other carbohydrates would surely be improved for the final industrial applications. In addition, based on the broad substrate specificities of PS, this systematic metabolic engineering strategy used for the *de novo* biosynthesis of D-panthenol could also be applied to the production of other valuable D-PA derivatives.

Author contributions

Zhiqiang Liu and Yuguo Zheng conceived and initiated the project. Junping Zhou, Zheng Zhang, Xinyuan Xin and Xueyun Feng wrote the paper and performed the experiments. Yihong Wang, Yinan Xue, Bo Zhang and Man Zhao reviewed this paper and provided valuable suggestions. All the authors read, edited, and approved the final manuscript.

Data availability

The data that support the findings of this study are available from the corresponding author upon reasonable request.

Conflicts of interest

All the authors declare no conflict of interest.

Acknowledgements

This work was supported by the National Key Research and Development Program of China (2022YFA0911800), National Natural Science Foundation of China (No. 32101170), the Key Research Development Program of Zhejiang Province (2024C03012) and 2023 Zhejiang Province postdoctoral research project preferential funding (ZJ2023159).

References

1 R. Padalkar, A. Madgulkar, R. Mate, A. Pawar, A. Shinde and S. Lohakare, *J. Drug Delivery Sci. Technol.*, 2024, **93**, 105390.
2 D. S. Semenovich, E. Y. Plotnikov, O. V. Titko, E. P. Lukiyenko and N. P. Kanunnikova, *Antioxidants*, 2021, **10**, 1699.
3 C. Tayman, U. Çakır, A. Kurt, Ö. Ertekin, T. T. Turkmenoglu, M. Çağlayan and E. Işık, *Biotech. Histochem.*, 2024, 1–9.
4 G. Blanchard, S. Kerre, A. Walker, E. Dendooven, O. Aerts, A. Goossens, M. Gilliet and T. Seremet, *Contact Dermatitis*, 2022, **87**, 468.
5 D. S. Semenovich, E. Y. Plotnikov, E. P. Lukiyenko, A. A. Astrowski and N. P. Kanunnikova, *Int. J. Mol. Sci.*, 2022, **23**, 12273.
6 J. Y. Shin, J. Kim, Y. Choi, N. Kang and S. Lee, *Curr. Issues Mol. Biol.*, 2021, **43**, 1361–1373.
7 G. Aquilina, A. Chesson, P. S. Cocconcelli, J. de Knecht, N. Dierick, M. A. Gralak, G. Bories, J. Gropp, I. Halle, C. Hogstrand, R. Kroker, L. Leng, A.-K. L. Haldorsen, S. L. Puente, A. Mantovani, G. Martelli, M. Mézes, D. Renshaw, M. Saarela, K. Sejrsen and J. Westendorf, *EFSA J.*, 2011, **9**, 2410.
8 P. Hu, X. Wu, Y. Zhang, M. Liu, Y. Tao, Z. Huang and F. Chen, *Green Chem.*, 2024, **26**, 2124–2134.
9 Y. Zhan, F. Zhou, W. Ruan, H. Yin, Z. Li, H. Wang, T. Li, D. Cai, S. Yang and X. Ma, *Green Chem.*, 2023, **25**, 8718–8729.
10 F. Song, Z. Qin, K. Qiu, Z. Huang, L. Wang, H. Zhang, X. Shan, H. Meng, X. Liu and J. Zhou, *Metab. Eng.*, 2024, **84**, 158–168.
11 X. Dong, C. Sun, J. Guo, X. Ma, M. Xian and R. Zhang, *Green Chem.*, 2023, **25**, 7662–7672.
12 W. J. Kim, Y. Lee, H. U. Kim, J. Y. Ryu, J. E. Yang and S. Y. Lee, *Cell Syst.*, 2023, **14**, 990–1001.
13 WO2022001939-A1; CN113846127-A; EP4174185-A1; US2023348941-A1; CN113846127-B; EP4174185-A4.
14 D. Chen, L. X. Xu, Y. Yu, Q. L. Mo, X. T. Qi and C. Liu, *Angew. Chem., Int. Ed.*, 2023, **62**, e202215168.
15 G. A. Strohmeier, E. I. C. Eiteljörg, A. Schwarz and M. Winkler, *Chem. – Eur. J.*, 2019, **25**, 6119–6123.

Published on 20 January 2025. Downloaded by Zhejiang University of Technology on 1/28/2025 6:21:55 AM.

16 L. N. Jayakody and Y. S. Jin, *Appl. Microbiol. Biotechnol.*, 2021, **105**, 2675–2692.
17 B. Zhang, X. M. Zhang, W. Wang, Z. Q. Liu and Y. G. Zheng, *Food Chem.*, 2019, **294**, 267–275.
18 S. P. Zou, Z. J. Wang, K. Zhao, B. Zhang, K. Niu, Z. Q. Liu and Y. G. Zheng, *Biotechnol. Appl. Biochem.*, 2021, **68**, 1227–1235.
19 S. P. Zou, K. Zhao, Z. J. Wang, B. Zhang, Z. Q. Liu and Y. G. Zheng, *3 Biotech*, 2021, **11**, 295.
20 B. Zhang, L. Chen, J. Y. Jin, N. Zhong, X. Cai, S. P. Zou, H. Y. Zhou, Z. Q. Liu and Y. G. Zheng, *Food Biosci.*, 2021, **43**, 101283.
21 S. P. Zou, K. Zhao, H. Tang, Z. Zhang, B. Zhang, Z. Q. Liu and Y. G. Zheng, *J. Biotechnol.*, 2021, **339**, 65–72.
22 B. Li, B. Zhang, P. Wang, X. Cai, Y. Q. Tang, J. Y. Jin, J. X. Liang, Z. Q. Liu and Y. G. Zheng, *Biotechnol. J.*, 2022, **17**, e2100431.
23 Y. H. Wang, J. P. Zhou, Z. Zhang, L. G. Huang, B. Zhang, Z. Q. Liu and Y. G. Zheng, *Bioresour. Technol.*, 2024, **411**, 131325.
24 X. Ding, W. Yang, X. Du, N. Chen, Q. Xu, M. Wei and C. Zhang, *Metab. Eng.*, 2023, **78**, 128–136.
25 P. H. Yuan, M. T. Xu, C. Y. Mao, H. Zheng and D. C. Sun, *ACS Synth. Biol.*, 2023, **12**, 2983–2995.
26 M. Z. Abidin, T. Saravanan, E. Strauss and G. J. Poelarends, *Org. Biomol. Chem.*, 2021, **19**, 4515–4519.
27 B. Li, B. Zhang, P. Wang, X. Cai, Y. Q. Tang, J. Y. Jin, J. X. Liang, Z. Q. Liu and Y. G. Zheng, *Biotechnol. J.*, 2022, **17**, 2100431.
28 Y. Y. Chen, L. G. Huang, T. Yu, Y. Yao, M. M. Zhao, A. P. Pang, J. P. Zhou, B. Zhang, Z. Q. Liu and Y. G. Zheng, *ACS Synth. Biol.*, 2024, **13**, 2457–2469.
29 S. Shapiro, *J. Antibiot.*, 2013, **66**, 371–386.
30 B. Zhang, R. Li, L. Yu, C. Wu, Z. Liu, F. Bai, B. Yu and L. Wang, *J. Agric. Food Chem.*, 2023, **71**, 11131–11140.
31 Y. Xi, H. Xu, T. Zhan, Y. Qin, F. Fan and X. Zhang, *Metab. Eng.*, 2023, **75**, 170–180.
32 T. Kogure, M. Suda, K. Hiraga and M. Inui, *Metab. Eng.*, 2021, **65**, 232–242.
33 M. Nie, J. Wang and K. Zhang, *Microb. Cell Fact.*, 2023, **22**, 138.
34 H. Mishima, H. Watanabe, K. Uchigasaki, S. Shimoda, S. Seki, T. Kumagai, T. Nochi, T. Ando and H. Yoneyama, *Microorganisms*, 2021, **9**, 472.
35 Y. Wang, X. Wang, G. Ma, L. Xie, D. Liu, Y. Wang, X. Zhao, Y. Su, A. V. Perepelov and P. Ding, *Green Chem.*, 2023, **25**, 4818–4832.
36 Y. Zhang, X. L. Wang, C. Odesanmi, Q. T. Hu, D. D. Li, Y. Tang, Z. Liu, J. Mi, S. W. Liu and T. Y. Wen, *Msystems*, 2024, **9**, e00839-23.
37 Y. S. Tan, G. Fuentes and C. Verma, *Proteins: Struct., Funct., Bioinf.*, 2011, **79**, 1715–1727.
38 K. S. Chakrabarti, K. G. Thakur, B. Gopal and S. P. Sarma, *FEBS J.*, 2010, **277**, 697–712.
39 R. F. Li, H. J. Wijma, L. Song, Y. L. Cui, M. Otzen, Y. E. Tian, J. W. Du, T. Li, D. D. Niu, Y. C. Chen, J. Feng, J. Han, H. Chen, Y. Tao, D. B. Janssen and B. Wu, *Nat. Chem. Biol.*, 2018, **14**, 664–670.
40 G.-F. Jin, J.-M. Tian, X.-Y. Liu, Z.-D. Chen, L.-T. Yan, S.-H. Hua, H. Liu, H.-J. Yang, H. Li and W.-Y. Gao, *Mol. Catal.*, 2023, **547**, 113286.
41 C. Y. Wang, Q. Y. Li, P. Zhou, X. J. Chen, J. P. Shi and Z. J. Zhao, *Microorganisms*, 2022, **10**, 1927.
42 T. S. R. Reddy, N. Ganesh, A. S. S. Pavan and S. Senthilkumar, *Bioprocess Biosyst. Eng.*, 2022, **45**, 843–854.
43 W. Li, H. Wu, M. Li and K. Y. San, *Biotechnol. Bioeng.*, 2018, **115**, 444–452.
44 Z. Jiang, Y. Jiang, H. Wu, W. Zhang, F. Xin, J. Ma and M. Jiang, *Bioengineering*, 2023, **10**, 881.
45 S. Li, Z. Ye, E. A. Moreb, J. N. Hennigan, D. B. Castellanos, T. Yang and M. D. Lynch, *Metab. Eng.*, 2021, **64**, 26–40.
46 C. Spry, K. Kirk and K. J. Saliba, *FEMS Microbiol. Rev.*, 2008, **32**, 56–106.
47 K. J. Saliba and C. Spry, *Biochem. Soc. Trans.*, 2014, **42**, 1087–1093.
48 S. B. Jilani, C. Dev, D. Eqbal, K. Jawed, R. Prasad and S. S. Yazdani, *Microb. Cell Fact.*, 2020, **19**, 1–13.
49 D. A. Smith, B. J. Nakamoto, M. K. Suess and M. L. Fogel, *Front. Microbiol.*, 2022, **13**, 840167.
50 P. Li, M. Wang, H. Di, Q. Du, Y. Zhang, X. Tan, P. Xu, C. Gao, T. Jiang and C. Lü, *Microb. Cell Fact.*, 2024, **23**, 49.
51 D. McCloskey, S. B. Xu, T. E. Sandberg, E. Brunk, Y. Hefner, R. Szubin, A. M. Feist and B. O. Palsson, *Appl. Environ. Microbiol.*, 2018, **84**, e00823-18.
52 T. Horinouchi, A. Sakai, H. Kotani, K. Tanabe and C. Furusawa, *J. Biotechnol.*, 2017, **255**, 47–56.
53 R. Kawai, Y. Toya, K. Miyoshi, M. Murakami, T. Niide, T. Horinouchi, T. Maeda, A. Shibai, C. Furusawa and H. Shimizu, *Biotechnol. Bioeng.*, 2022, **119**, 936–945.
54 S. Wang, Y. Y. Wang, Q. Y. Yuan, L. Yang, F. G. Zhao, Y. Lin and S. Y. Han, *Green Chem.*, 2023, **25**, 8845–8857.
55 T. Horinouchi, T. Maeda and C. Furusawa, *World J. Microbiol. Biotechnol.*, 2018, **34**, 1–9.
56 Z. Tan, J. M. Yoon, D. R. Nielsen, J. V. Shanks and L. R. Jarboe, *Metab. Eng.*, 2016, **35**, 105–113.
57 Z. Tan, P. Khakbaz, Y. Chen, J. Lombardo, J. M. Yoon, J. V. Shanks, J. B. Klauda and L. R. Jarboe, *Metab. Eng.*, 2017, **44**, 1–12.

 This journal is © The Royal Society of Chemistry 2025